

Manipulating Gloss of Real Objects Under Omnidirectional Lighting

Yuki Miyoshi¹, Ryo Kawahara²^a and Takahiro Okabe³^b

¹Department of Artificial Intelligence, Kyushu Institute of Technology, Iizuka, Fukuoka 820-8502, Japan

²Graduate School of Informatics, Kyoto University, Sakyo-ku, Kyoto 606-8501, Japan

³Information Technology Track, Okayama University, Kita-ku, Okayama 700-8530, Japan

Keywords: Gloss Manipulation, Omnidirectional Lighting Environment, Specular Reflection, Polarization.

Abstract: Manipulating the appearances of real-world objects by using active illumination is useful for XR. In this paper, we propose a method for manipulating the gloss of real objects observed by our naked eyes under omnidirectional lighting environments. Our proposed method makes use of the fact that specular reflection components are sensitive to the polarization state of the incident light and the high-frequency components of the illumination environment, while diffuse reflection components are insensitive to them. Specifically, our method optimizes the polarization angles and intensities of incident lighting environments for manipulating the gloss of real objects. We build a lighting system by using a dome screen and two pairs of a projector and a transmissive LC panel for controlling both the polarization angles and high-frequency components of incident lighting environments. We conduct a number of experiments, and show that our method achieves the gloss manipulation without using the geometric and photometric properties of an object of interest.

1 INTRODUCTION

The appearance of an object depends not only on the geometric and photometric properties of the object but also on the light sources illuminating it. Manipulating the appearances of real-world objects by using active illumination such as a projector and a light stage is useful for XR (extended reality/cross reality). In this paper, we focus on the gloss manipulation of real objects under omnidirectional lighting environments.

A projector (or a projector-camera system) is useful for manipulating the appearance of an object, in particular for relighting and material editing (Raskar et al., 2001; Siegl et al., 2015). This is because a projector can *pixel-wisely* illuminate the object: it can illuminate each point on the object surface with different intensities and colors. Unfortunately, however, the appearance manipulation using a projector-camera system requires the geometric and photometric properties of an object of interest or the light transport of a scene.

On the other hand, a light stage is useful for reproducing the appearance of an object under omni-

directional lighting environments without using the geometric and photometric properties of the object (Debevec et al., 2002; Wenger et al., 2005; Debevec, 2012). Unfortunately, however, it is difficult to manipulate the reflectance properties of the object, since each light source illuminates the *entire* object. Ma et al. (Ma et al., 2007) capture the specular-free images under omnidirectional lighting environments by using a light stage with fixed linear polarizers and a camera with a linear polarizer. However, the gloss manipulation (emphasis and suppression) observed by our naked eyes is still an open problem to be addressed.

In this paper, we propose a method for manipulating the gloss of real objects observed by our naked eyes under omnidirectional lighting environments. The key idea of our proposed method is the use of polarized and high-frequency illumination. Specifically, we make use of the fact that specular reflectance is maximal/minimal when the polarization direction is perpendicular/parallel to the outgoing plane, but the diffuse reflectance is almost constant according to the Fresnel equations (Shurcliff, 1962; Wolff, 1990). In addition, we utilize the fact based on the frequency analysis of reflection that specular/diffuse reflection components are sensitive/insensitive to the high-frequency components of an illumination distribution (Ramamoorthi and Hanrahan, 2001b).

^a <https://orcid.org/0000-0002-9819-3634>

^b <https://orcid.org/0000-0002-2183-7112>

To control the intensity/color and polarization angle of the incident light coming from each direction, we build a programmable omnidirectional lighting system by using a dome screen and two pairs of a projector and a transmissive liquid crystal (LC) panel. The projectors and the LC panels are used for controlling the color/intensity and the polarization angle respectively. Our proposed method manipulates the gloss of real objects on the basis of the lookup table constructed using a reference object with the same refractive index as an object of interest without using the geometric and photometric properties of the object.

The main contributions of this study are threefold. First, we propose a novel framework for manipulating the gloss of real objects observed by our naked eyes under omnidirectional lighting environments on the basis of the polarized and high-frequency illumination. Second, we build a novel lighting system by using a dome screen and two pairs of a projector and a transmissive LC panel for controlling both the polarization angles and high-frequency components of incident lighting environments. Third, we achieve the gloss manipulation without using the geometric and photometric properties of an object of interest by using a reference object and a lookup table.

2 PROPOSED METHOD

2.1 Lighting System

Figure 1 shows our setup using two pairs of a projector and a transmissive LC panel¹, a dome screen, and a color camera. First, the light ray emitted from the projector passes through the transmissive LC panel. Second, it is reflected on the dome screen and incident to a target object. Third, it is reflected on the surface of the target object, and finally the reflected light is observed by the camera. We assume that the dome screen is distant from the target object, and denote the direction of the incident light seen from the object by (θ, ϕ) . Here, θ and ϕ are the zenith and azimuth angles of the global spherical coordinate system whose pole is the camera direction.

The projector controls the per-pixel intensity of the light ray. The front linear polarizer of the transmissive LC panel is removed, and then it controls the per-pixel angle of linear polarization. In addition, the polarization-preserving material is painted on the dome screen. Thus, our lighting system enables us to

¹We explain the reason why the two pairs are required in Section 3.2.

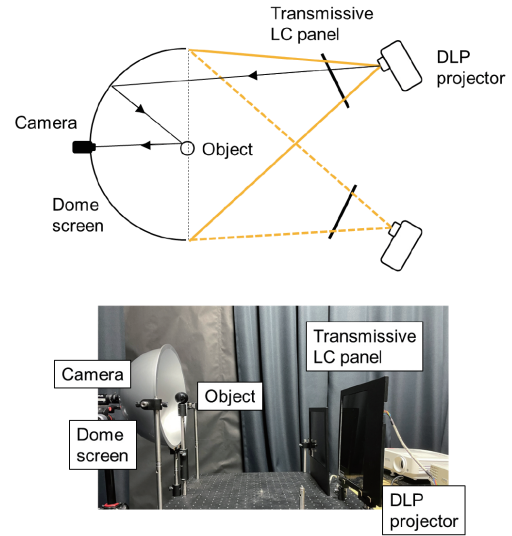


Figure 1: Our setup using two pairs of a projector and a transmissive LC panel, a dome screen, and a color camera.

control the intensity $L(\theta, \phi)$ and the angle of linear polarization $\omega(\theta, \phi)$ of the light ray coming from (θ, ϕ) to the target object.

2.2 Manipulation

Let us consider a mirror surface that reflects the light ray coming from the direction (θ, ϕ) to the camera. Since the light ray is reflected to the direction of the mirror reflection, the surface normal is represented as $(\theta/2, \phi)$ by using the spherical coordinate system. In other words, the incident angle to the mirror surface is $\theta/2$. We denote $\theta/2$ by θ' hereafter.

It is known that the specular reflectance is maximal/minimal when the polarization direction is perpendicular/parallel to the outgoing plane spanned by the surface normal and the direction of the reflected light, *i.e.* the s-polarized light/p-polarized light (Shurcliff, 1962; Wolff, 1990). Therefore, the intensity of the reflected light $I(\theta, \phi)$ illuminated by unpolarized light is described by

$$I(\theta, \phi) = L(\theta, \phi)\bar{R}(\theta'). \tag{1}$$

Here, $\bar{R}(\theta')$ is the average of the maximal reflectance $R_s(\theta')$ and the minimal reflectance $R_p(\theta')$:

$$\bar{R}(\theta') = \frac{R_s(\theta') + R_p(\theta')}{2}. \tag{2}$$

Our proposed method manipulates the gloss of real object under omnidirectional lighting by controlling the intensity and the angle of linear polarization. Specifically, we add the linear combination of spheri-

cal harmonics to the intensity as

$$L'(\theta, \phi) = L(\theta, \phi) + \sum_{k=0}^K \sum_{m=-k}^k a_{km} Y_{km}(\theta, \phi), \quad (3)$$

where $Y_{km}(\theta, \phi)$ is the spherical harmonics of the k -th degree and the m -th order and a_{km} is its coefficient of the linear combination. We denote the reflectance depending on the angle of linear polarization $\omega(\theta, \phi)$ by $R(\theta', \omega(\theta, \phi))$.

Therefore, the intensity of the reflected light $I'(\theta, \phi)$ after manipulation is described by

$$\begin{aligned} I'(\theta, \phi) &= L'(\theta, \phi) R(\theta', \omega(\theta, \phi)) \\ &= \left[L(\theta, \phi) + \sum_{k=0}^K \sum_{m=-k}^k a_{km} Y_{km}(\theta, \phi) \right] \\ &\quad \times R(\theta', \omega(\theta, \phi)). \end{aligned} \quad (4)$$

Our proposed method controls the coefficients of the linear combination a_{km} ($k = 1, 2, 3, \dots, K, |m| \leq k$) and the angle of linear polarization $\omega(\theta, \phi)$ so that the gloss, *i.e.* specular reflection components observed on the target object is emphasized or suppressed as expected.

2.3 Optimization

We denote the target ratio, *i.e.* the desired ratio of the emphasized/suppressed intensity and the original intensity of gloss (specular reflection components) by t . Our proposed method controls the coefficients of the linear combination a_{km} and the angle of linear polarization $\omega(\theta, \phi)$ so that

$$t \simeq \frac{I'(\theta, \phi)}{I(\theta, \phi)} \quad (5)$$

for all surface normals (θ', ϕ) or equivalently for all lighting directions (θ, ϕ) .

In addition, our proposed method considers two penalty terms. The first one termed F_1 is the penalty on negative lighting intensities:

$$F_1(\theta, \phi) = \max(-L'(\theta, \phi), 0). \quad (6)$$

The second one termed F_2 is the penalty on the change in diffuse reflection components:

$$F_2 = \sum_{k=0}^K \sum_{m=-k}^k \beta_k |a_{k,m}|. \quad (7)$$

Here, β_k is the Fourier spectrum of the Lambertian kernel; it represents the contribution of the $Y_{km}(\theta, \phi)$ to the diffuse reflection components. It is known that the first nine low-frequency terms, *i.e.* $k = 0, 1, 2$ explain the power of 99.2% of diffuse reflection components (Ramamoorthi and Hanrahan, 2001a).

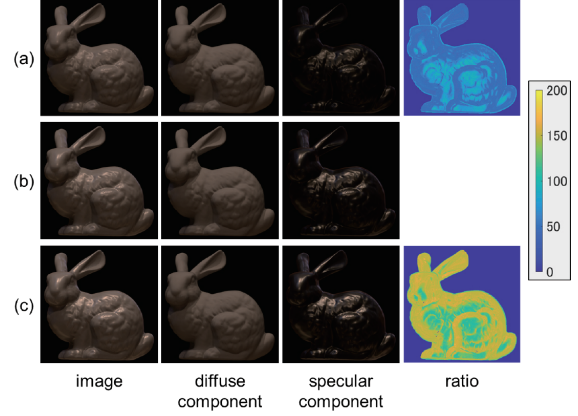


Figure 2: The results for the Stanford Bunny: (a) gloss suppression ($t = 0.5$), (b) original, and (c) gloss emphasis ($t = 1.5$) from top to bottom.

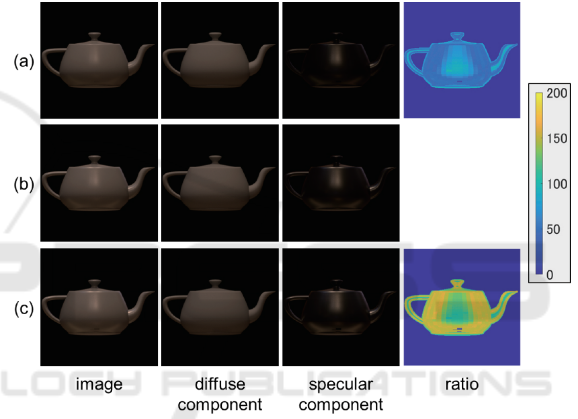


Figure 3: The results for the Utah Teapot: (a) gloss suppression ($t = 0.5$), (b) original, and (c) gloss emphasis ($t = 1.5$) from top to bottom.

Thus, our proposed method results in the following optimization:

$$\begin{aligned} \min_{\mathbf{a}, \boldsymbol{\omega}} \quad & \sum_{\theta, \phi} \left[\frac{L'(\theta, \phi) R(\theta', \omega(\theta, \phi))}{L(\theta, \phi) \bar{R}(\theta')} - t \right]^2 \\ & + \lambda_1 \sum_{\theta, \phi} F_1(\theta, \phi) + \lambda_2 F_2. \end{aligned} \quad (8)$$

Here, $\mathbf{a} = (a_{00}, a_{1-1}, a_{10}, a_{11}, \dots)$ and $\boldsymbol{\omega}$ is the set of the polarization angles for each lighting direction (θ, ϕ) . We denote the weights of the second and third terms by λ_1 and λ_2 respectively. We solve the above minimization via alternative optimization; we iteratively fix one of the \mathbf{a} and $\boldsymbol{\omega}$ and optimize the other.

Note that our proposed method is applicable to rough surfaces although the above derivation assumes the mirror surface. This is because we can assume that rough surfaces consist of the micro-facets of mirrors with various surface normals, and the first term

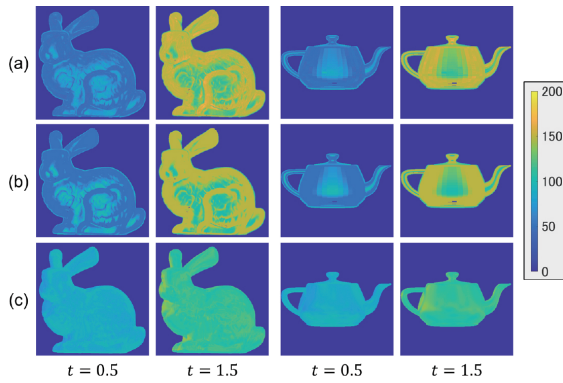


Figure 4: The ablation study for the Stanford Bunny (left) and the Utah Teapot (right): (a) ours, (b) ours w/o high-freq., and (c) ours w/o polarized from top to bottom.

in eq.(8) impose that the ratios for the all surface normals are close to the target ratio t .

3 EXPERIMENTS

3.1 Synthetic Images

First, we conducted the experiments using synthetic images, for which the ground truth of diffuse and specular reflection components are known, in order to confirm the effectiveness of our proposed method both qualitatively and quantitatively.

Setup:

We used the Stanford Bunny and the Utah Teapot for the target objects and the Grace Cathedral from the light probe image gallery (Debevec, 1998) for the lighting environment. We used Mitsuba 3 for rendering images. We solved the minimization problem of eq.(8) by using the trust region reflective algorithm (Coleman and Li, 1996) (MATLAB function of lsqnonlin). We set the weights in eq.(8) as $\lambda_1 = 10^4$ and $\lambda_2 = 5 \times 10^4$ respectively.

Results:

Figure 2 shows the results for the Stanford Bunny: the output images, the diffuse reflection components, the specular reflection components, and the ratios (%) of the suppressed/emphasized specular reflection components and the original ones from left to right. Comparing (a) gloss suppression ($t = 0.5$), (b) original, and (c) gloss emphasis ($t = 1.5$), we can qualitatively see that our proposed method suppresses/emphasizes specular reflection components as expected while it preserves diffuse reflection components. We can also see that the accuracy of gloss manipulation is relatively low for points with surface normals toward the camera direction. This is because the degree of lin-

Table 1: The quantitative evaluation for the Stanford Bunny.

	$t = 0.5$		$t = 1.5$	
	Specular (ratio)	Diffuse (SSIM)	Specular (ratio)	Diffuse (SSIM)
Ours	58.89%	0.99997	140.97%	0.99998
Ours w/o high-freq.	61.50%	1.00000	137.79%	1.00000
Ours w/o polarized	91.73%	0.99991	108.61%	0.99991

Table 2: The quantitative evaluation for the Utah Teapot.

	$t = 0.5$		$t = 1.5$	
	Specular (ratio)	Diffuse (SSIM)	Specular (ratio)	Diffuse (SSIM)
Ours	59.42%	1.00000	138.93%	1.00000
Ours w/o high-freq.	61.49%	1.00000	136.49%	1.00000
Ours w/o polarized	91.31%	0.99997	108.08%	0.99997

ear polarization is low for those points, and the effect of polarized incident light is somewhat limited. We can see that we obtain the similar results for the Utah Teapot as shown in Figure 3.

Figure 4 (left) and Table 1 shows the qualitative and quantitative evaluation of our proposed method for the Stanford Bunny. We can see that our method works well; the ratios of the suppressed/emphasized specular reflection components and the original ones are almost the same as the target values: $t = 0.5$ (50%) and $t = 1.5$ (150%). We can see that our method works better than the use of only one of the polarized illumination (Ours w/o high-freq.) and high-frequency illumination (Ours w/o polarized). We can see that we obtain the similar results for the Utah Teapot as shown in Figure 4 (right) and Table 2.

3.2 Real Images

Second, we conducted the experiments using real images, for which the ground truth of diffuse and specular reflection components are unknown, in order to confirm the effectiveness of our proposed method on real images qualitatively.

Setup:

We used two pairs of a projector of MS524 from BenQ and a transmissive LC panel, *i.e.* an LC panel of JTP121LKNN from JNM Display without a front polarization filter and a color camera of BFS-U3-51S5PC-C from FLIR. We used two transmissive LC panels because the range of the polarization angles of each LC panel is at most 90° as shown in Figure 5. Then, we rotated one of the LC panel 90° so that the two LC panels covers the polarization angles from 0° to 180° .

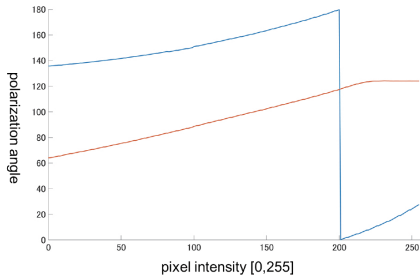


Figure 5: The polarization angles vs. the input pixel values to the transmissive LC panels; the red and blue lines stand for the polarization angle of the first and the second LC panels. Note that the second LC panel is rotated 90° .

We conducted the geometric calibration of our setup by using a mirror sphere. Specifically, we estimated the correspondence between the projector pixel, the LC panel pixel, and (θ, ϕ) by using structured light patterns.

We conducted the photometric calibration of our setup by using a reference object with known shape; we used a smooth specular sphere without diffuse reflection components. Because the light rays incident to an object surface from our lighting system is not completely polarized but partially polarized, we made the lookup table between the input pixel value to the LC panel and $R(\theta', \omega(\theta, \phi))$. Note that our proposed method based on the above photometric calibration is applicable to convex objects with the same refractive index as the reference object.

In the same manner as the experiments using synthetic images, we solved the minimization problem of eq.(8) by using the trust region reflective algorithm. We set the weights in eq.(8) as $\lambda_1 = 10^4$ and $\lambda_2 = 5 \times 10^4$ respectively.

Results:

Figure 6 shows the results for the plastics toys: (a) bird, (b) bear, and (c) octopus under the illumination environment of the Grace Cathedral. The green and blue images under the suppressed and emphasized images show the difference images from the original ones; we represent the positive/negative pixel values as B/G channels. We multiply the pixel values of the difference images by 5 for display purpose.

We can qualitatively see that our proposed method suppresses/emphasizes specular reflection components as expected. Note that we achieve such gloss manipulation without using the geometric and photometric properties of the target objects. We can also see that some artifacts are slightly visible due to cast shadows caused at concave areas.

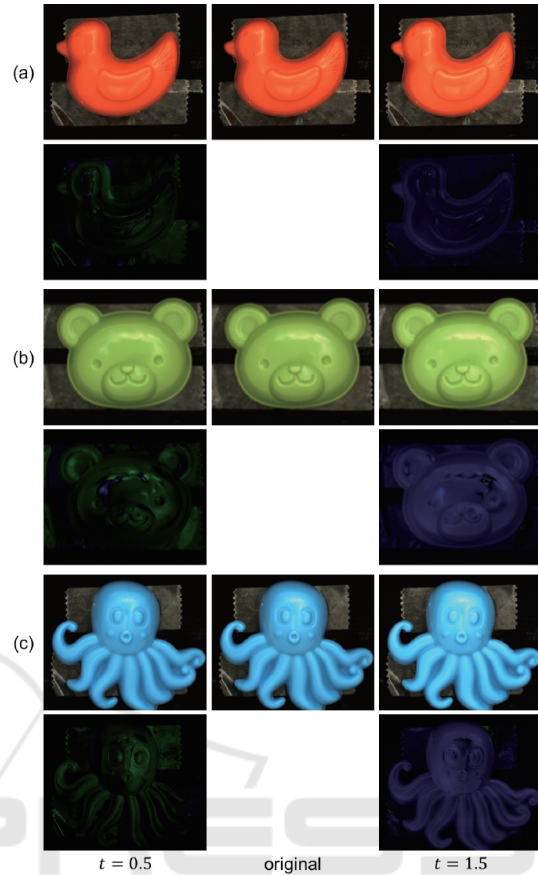


Figure 6: The results using real images of the plastics toys: (a) bird, (b) bear, and (c) octopus.

4 CONCLUSION

We proposed a novel framework for manipulating the gloss of real objects observed by our naked eyes under omnidirectional lighting environments on the basis of the polarized and high-frequency illumination. In order to control both the polarization angles and high-frequency components of incident lighting environments, we built a novel lighting system by using a dome screen and two pairs of a projector and a transmissive LC panel. We conducted a number of experiments using both synthetic and real images, and confirmed the effectiveness of our method.

One of the limitations of our proposed method is the assumption of convex objects, *i.e.* no cast shadows are observed on the objects' surfaces. Another limitation is the inter-reflection caused on the concave screen. To cope with those limitations is the future work of this study.

ACKNOWLEDGEMENTS

This work was supported by JSPS KAKENHI Grant Numbers JP20H00612 and JP22K17914.

REFERENCES

- Coleman, T. F. and Li, Y. (1996). An interior trust region approach for nonlinear minimization subject to bounds. *SIAM Journal on Optimization*, 6(2):418–445.
- Debevec, P. (1998). Rendering synthetic objects into real scenes: bridging traditional and image-based graphics with global illumination and high dynamic range photography. In *Proceedings of the 25th Annual Conference on Computer Graphics and Interactive Techniques*, pages 189–198.
- Debevec, P. (2012). The Light Stages and Their Applications to Photoreal Digital Actors. In *In Proc. SIGGRAPH Asia2012, Technical Briefs*.
- Debevec, P., Wenger, A., Tchou, C., Gardner, A., Waese, J., and Hawkins, T. (2002). A lighting reproduction approach to live-action compositing. *ACM Trans. Graph.*, pages 547–556.
- Ma, W.-C., Hawkins, T., Peers, P., Chabert, C.-F., Weiss, M., and Debevec, P. (2007). Rapid acquisition of specular and diffuse normal maps from polarized spherical gradient illumination. In *Proceedings of the 18th Eurographics Conference on Rendering Techniques*, pages 183–194.
- Ramamoorthi, R. and Hanrahan, P. (2001a). On the relationship between radiance and irradiance: determining the illumination from images of a convex lambertian object. *J. Opt. Soc. Am. A*, 18(10):2448–2459.
- Ramamoorthi, R. and Hanrahan, P. (2001b). A signal-processing framework for inverse rendering. In *Proceedings of the 28th Annual Conference on Computer Graphics and Interactive Techniques*, page 117–128.
- Raskar, R., Welch, G., Low, K.-L., and Bandyopadhyay, D. (2001). Shader lamps: Animating real objects with image-based illumination. In *In Proc. EGSR2001*, pages 89–102.
- Shurcliff, W. (1962). *Polarized Light: Production and Use*. Harvard University Press.
- Siegl, C., Colaianni, M., Thies, L., Thies, J., Zollhöfer, M., Izadi, S., Stamminger, M., and Bauer, F. (2015). Real-time pixel luminance optimization for dynamic multi-projection mapping. *ACM Trans. Graph.*, 34(6).
- Wenger, A., Gardner, A., Tchou, C., Unger, J., Hawkins, T., and Debevec, P. (2005). Performance relighting and reflectance transformation with time-multiplexed illumination. *ACM Trans. Graph.*, 24(3):756–764.
- Wolff, L. (1990). Polarization-based material classification from specular reflection. *IEEE Trans. PAMI*, 12(11):1059–1071.